ISSN 1063-780X, Plasma Physics Reports, 2007, Vol. 33, No. 11, pp. 956–960. © Pleiades Publishing, Ltd., 2007.
Original Russian Text © N.V. Denisova, S.S. Katsnelson, G.A. Pozdnyakov, 2007, published in Fizika Plazmy, 2007, Vol. 33, No. 11, pp. 1042–1047.

PLASMA DIAGNOSTICS

Computer Tomography Imaging of Fast Plasmachemical Processes

N. V. Denisova, S. S. Katsnelson, and G. A. Pozdnyakov

Khristianovich Institute of Theoretical and Applied Mechanics, Siberian Branch, Russian Academy of Sciences, Institutskaya ul. 4/1, Novosibirsk, 630090 Russia

Received March 13, 2007

Abstract—Results are presented from experimental studies of the interaction of a high-enthalpy methane plasma bunch with gaseous methane in a plasmachemical reactor. The interaction of the plasma flow with the rest gas was visualized by using streak imaging and computer tomography. Tomography was applied for the first time to reconstruct the spatial structure and dynamics of the reagent zones in the microsecond range by the maximum entropy method. The reagent zones were identified from the emission of atomic hydrogen (the H_α line) and molecular carbon (the Swan bands). The spatiotemporal behavior of the reagent zones was determined, and their relation to the shock-wave structure of the plasma flow was examined.

PACS numbers: 82.33.Xj, 52.70.-m

DOI: 10.1134/S1063780X07110074

1. INTRODUCTION

In recent years, fundamental studies of the interaction of high energy density flows (in particular, high-enthalpy plasma flows) with matter have attracted much attention. Interest in these studies stems from possible applications of such flows in plasma- and nanotechnologies. Previous studies on electrodynamic plasma acceleration resulted in the creation of high-enthalpy plasma sources capable of operating in a wide parameter range. Further development of these studies requires a more thorough investigation of the processes occurring in plasmachemical reactors.

Here, we present results from studies of the interaction of a high-enthalpy methane plasma flow with the rest gas (also methane) in a plasmachemical reactor. The plasma was produced by a high-power pulsed discharge and was accelerated by a magnetic field to a supersonic speed of about 5 km/s. The diameter of the plasma flow was 2 cm; i.e., the degree of plasma energy accumulation was very high. Such plasma flows interact with the rest gas on a microsecond time scale. Studies of the interaction dynamics of plasma flows with the rest gas are very important for understanding and controlling fast processes in plasmachemical reactors; however, they can only be performed within an approach that combines optical diagnostics based on high-speed photorecording and mathematical methods of computer tomography. Photorecording provides volume-integrated plasma emission characteristics. An important advantage of this technique is that it is nonintrusive; i.e., it does not perturb the plasma parameters. The algorithms of computer tomography allow one to calculate local emission coefficients. Under thermodynamic equilibrium conditions, these coefficients are related via the Boltzmann and Saha formulas to the electron temperature and density. In a nonequilibrium plasma, they are proportional to the local densities of emitting atoms and ions in certain excited states. In plasmachemical reactors, the distributions of the emission coefficients of the plasma components characterize the spatial structure of the reagent zones.

Modern algorithms and methods of computer tomography allow one to reconstruct the spatial distributions of the plasma parameters, including their fine internal structure. Computer tomography is a powerful diagnostic tool for studying both high- and low-temperature plasmas. At present, soft X-ray tomography used to investigate high-temperature plasma in tokamaks and stellarators is most thoroughly developed. In most experiments carried out with low-temperature plasmas, the plasma column is axisymmetric, so a single observation direction is enough to reconstruct its spatial structure. In some experiments, however, the plasma is asymmetric; therefore, great effort has been expended to develop algorithms and methods for reconstructing the fine structure of such plasmas. For plasmas in which axial symmetry is disturbed only slightly, the spatial distributions of the parameters can be reconstructed using a small number of observation directions. For example, in [1], the spatial distribution of the excited Hg atoms emitting at the 546.1-nm wavelength in a high-frequency electrodeless discharge was reconstructed tomographically by using an algorithm based on the maximum entropy method. It was found that, over the entire range of the discharge parameters under study, the density of emitting 7^3S Hg atoms was minimum at the center and maximum near the lamp wall. In [2], tomography was applied to reconstruct the electron density distribution in a laser plasma in the presence of a magnetic field. It was assumed that axial symmetry was disturbed only slightly, so the distribution was reconstructed by using two mutually perpendicular projections. In [3], tomography was used to reconstruct the distribution of the Cr atomic density in an arc plasma.

In the present study, optical tomography is applied to reconstruct the spatiotemporal distribution of the emission coefficients of atomic hydrogen (the H_α line) and C_2 molecules (the Swan bands) in a plasmachemical reactor by using an algorithm based on the maximum entropy method. The algorithm was developed in [4, 5] and was tested in numerical simulations and experiments. The calculations show that, the algorithm provides quite good reconstruction even when the number of observation directions is small. Here, it is used to reconstruct the spatial structure of an axisymmetric source by using one observation direction.

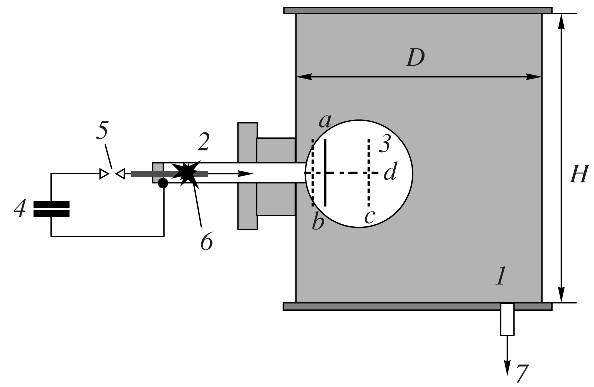

Fig. 1. Schematic of the experimental setup: (*1*) cylindrical chamber, (*2*) Marshall gun, (*3*) optical window, (*4*) capacitor bank, (*5*) controlled switch gap, (*6*) plasma, and (*7*) pumping out.

2. EXPERIMENTAL SETUP

A schematic of the experimental setup is shown in Fig. 1. The processes occurring in 350-mm-diameter 400-mm-high sealed cylindrical reactor chamber *1* were monitored through optical window *3* with a clear aperture of 100 mm. The plasma was accelerated by coaxial electrodynamic accelerator (Marshall gun) *2*, which generated plasma bunches with velocities from several km/s to a few tens of km/s, the initial gas pressure being up to a few kilopascals. The inner diameter of the 300-mm-long channel of the plasma accelerator was 20 mm. Capacitor bank *4* with a capacitance of 6.6-μF and charge voltage of 30 kV was connected to the Marshall gun via controlled switch gap *5*. The device operated as follows. The working volume was evacuated via pipe *7* to pressures lower than 5 Pa and was then filled with natural gas (a methane–ethane mixture also containing other hydrocarbons) at a pressure of 250 Pa. The capacitor bank was charged, and the measurement equipment was prepared for a shot. The discharge of the capacitor bank generated plasma *6*, which was accelerated to a high speed by the electrodynamic force. Then, the accelerated plasma bunch, at the front of which a compression shock formed, entered the working volume filled with natural gas. The propagation of a high-enthalpy plasma flow through the rest gas was accompanied by various shock, thermal, plasmachemical, and emission processes developing on a microsecond time scale. The aim of the present study was to investigate the spatiotemporal behavior of a fast plasma jet injected in a chemically active medium. By recording and analyzing the emission spectrum and spatial distribution of the emission coefficients in different spectral ranges, we determined the spatial structure and characteristic time of the processes under study.

In our experiments, we recorded the emission spectrum from the reaction zone, performed streak imaging of the interaction process, and measured the accelerator voltage and current. The time-integrated radiation spectrum emitted from a 1-mm-wide 80-mm-high region located at a distance of 15 mm from the end of the accelerator channel (Fig. 1, line *a*) was recorded by a crossed-dispersion spectrograph. The image of the emission zone was projected onto the spectrograph entrance slit. This allowed us to study the emission spectrum as a function of the distance from the accelerator axis. The center of the measurement region was at the channel axis.

Streak images were taken with slits oriented across and along the accelerator axis. The positions of the two end cross sections used for reconstruction (in total, 13 transverse cross sections were used) are shown by dashed lines *b* and *c* in Fig. 1. The slit oriented along the axis is marked by *d*. In the latter case, the emission from the paraxial region of the plasma flow propagating along the accelerator axis was recorded. The streak image thus obtained was used to synchronize streak images recorded with transversely oriented slits. Such a synchronization was necessary for tomographic reconstruction of the radial propagation of the emitting regions at different distances from the end of the accelerator channel. The transverse cross sections were spaced a distance of 5 mm from one another. The reproducibility of the process from shot to shot was high enough to perform tomographic reconstruction by using streak images obtained in different shots.

3. EXPERIMENTAL RESULTS

The time-integrated emission spectrum is shown in Fig. 2. The Roman numerals on the left show the diffraction orders of the spectrum. In the fourth order, there are the H_α line ($\lambda = 656$ nm) and the Swan band with the edge at $\lambda = 560$ nm (*a*). In the fifth order, there are the Swan band with the edge at $\lambda = 520$ nm (*b*), the H_β line, the Swan blue band (*c*), and the H_γ line. Thus, only atomic hydrogen and C_2 molecules emit in the visible range. This feature of the emission spectrum allows

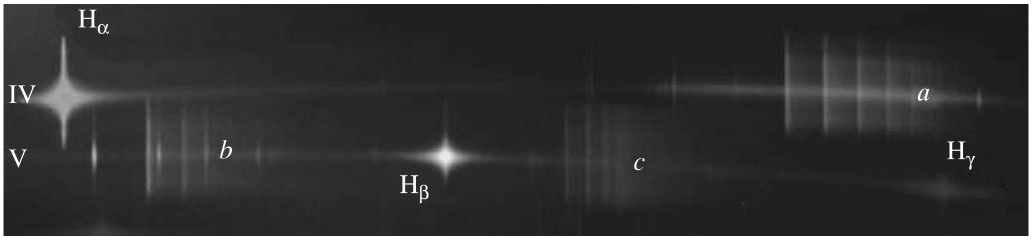

Fig. 2. Emission spectrum.

one to determine the distribution of the emission intensity of hydrogen atoms (the H_α red line) and carbon molecules C_2 (the Swan green band) by photorecording on a color film.

The lines emitted from the paraxial zone of the flow are highly broadened. The brightness and width of the hydrogen lines decrease rapidly with distance from the axis, whereas those of the Swan bands vary only slightly. The measurements of the half-width of the H_β line and the intensity ratio between the H_β and H_α lines showed that the electron temperature and density near the axis were $T \approx 10^4$ K and $n_e = (1 \pm 0.2) \times 10^{16}$ cm^{-3}, respectively.

Typical streak images taken with two mutually perpendicular orientations of the slits are shown in Figs. 3 and 4. Figure 3 shows a longitudinal streak image taken along the axis of the plasma flow, while Fig. 4 shows a transverse streak image taken in one (specifically, ninth) of the 13 transverse cross sections located consecutively along the axis.

4. TOMOGRAPHIC RECONSTRUCTION

The problem of visualization of the interaction of a plasma flow with a rest gas is reduced to tomographic reconstruction of the spatiotemporal evolution of the plasma emission characteristics. The absorption coefficients of the H_α line and the Swan green bands of molecular carbon are very small because hydrogen and molecular carbon are almost absent in the cold gas and the length of the hot region is smaller than the characteristic free paths of photons with the corresponding wavelengths. In this case, the radiative transfer equation takes the form

$$I_\lambda(p, \theta) = \int_{-\infty}^{\infty} \varepsilon_\lambda(x, y) dl_{p,\theta}, \quad (1)$$

where p and θ are the normal coordinates of chord l oriented along the line of sight. In our case, $I_\lambda(p, \theta)$ is the integral (along the line of sight) emission intensity at the wavelengths of the H_α line and Swan green bands and $\varepsilon_\lambda(x, y)$ is the corresponding local emissivity. Thus, the problem of tomographic reconstruction is to determine the distribution of $\varepsilon_\lambda(x, y)$ from the measured integral quantities $I_\lambda(p, \theta)$. From the mathematical standpoint, it is reduced to solving a Fredholm integral equation of the first kind. Since this problem belongs to the class of ill-posed inverse problems, it is often rather difficult to solve. There are various algorithms and methods for determining the maximum probable estimates of the solutions to such problems. A promising method is reconstruction based on the maximum entropy method, which was discussed in detail in [4, 5]. As was noted above, this algorithm was designed to study

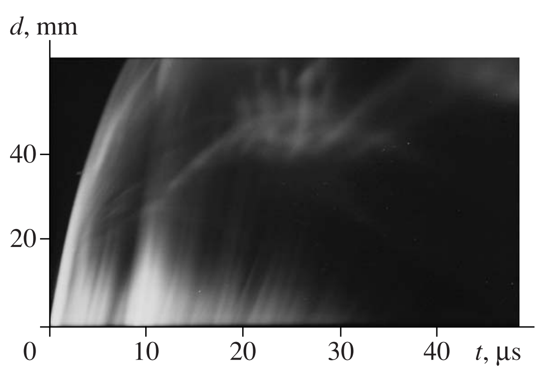

Fig. 3. Longitudinal streak image.

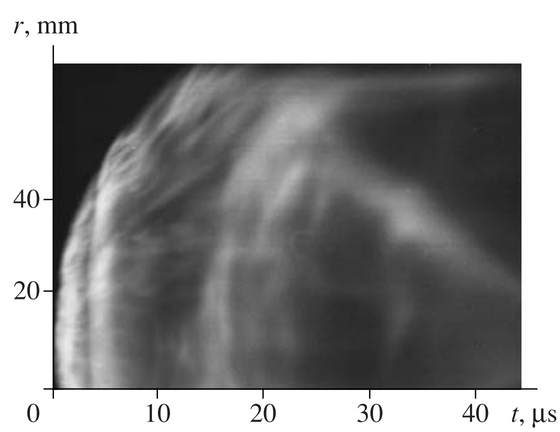

Fig. 4. Transverse streak image.

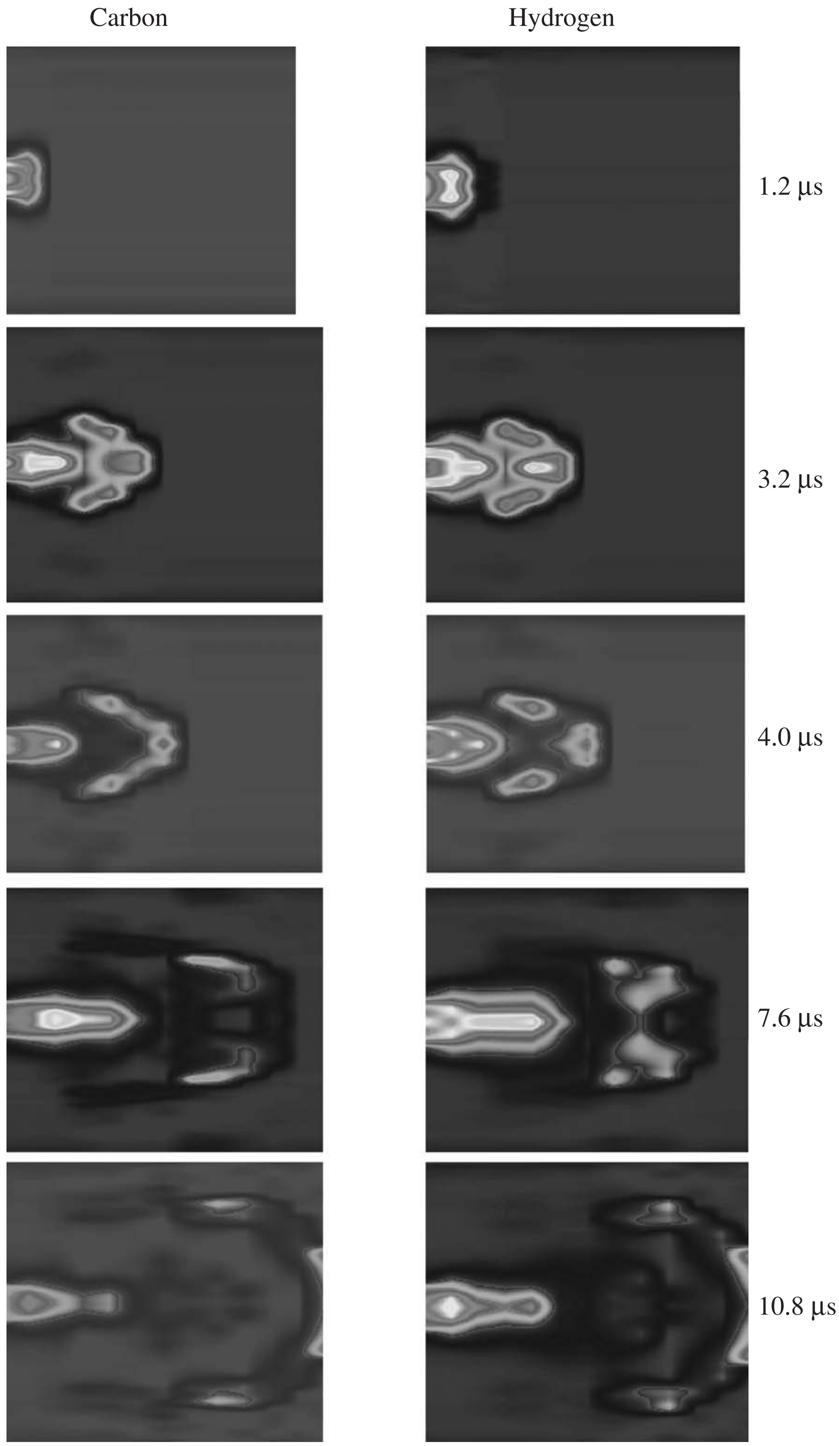

Fig. 5. Tomographic reconstruction of the spatial distribution of the emission coefficients of atomic hydrogen (right column) and molecular carbon (left column) in the central cross section of the plasmachemical reactor.

asymmetric plasma objects. In the present study, however, it is employed to reconstruct the spatial structure of an axisymmetric source.

The reconstruction was performed in Cartesian coordinates $\{x, y, z\}$ within a normalized domain $\{-1 \le x \le 1; -1 \le y \le 1; -1 \le z \le 1\}$, which was divided into $101 \times 101 \times 13$ voxels. The z axis was oriented along the plasma flow and coincided with the symmetry axis. We used a layer-by-layer method of 3D reconstruction: the reconstruction region was divided along the z axis into 13 layers corresponding to the 13 cross sections in which the measurements were performed. Each layer was marked with a number k: $z = z_k$, $k = 1, 2, 3, \ldots, 13$. The projection data were given by the corresponding column of a two-dimensional matrix $I_k(x)$. Since the streak images were synchronized, the columns with the same number in each of the 13 two-dimensional matrixes provided two-dimensional projection data for the reconstruction of a 3D object at a given instant t.

The reconstruction was performed by using color streak images, which demonstrated a fairly high axial symmetry of the plasma flow. An analysis of the red and green spectral regions allowed us to reconstruct the spatial distributions of the local emission coefficients of atomic hydrogen (H_α line) and C_2 molecules (Swan bands). Figure 5 presents the results of tomographic reconstruction—the spatial distributions of the emission coefficients of atomic hydrogen and molecular carbon in the central cross section of the plasmachemical reactor. These distributions indicate the reaction zones and illustrate their time evolution. The plasma bunch propagates from left to right. Note that the distributions of the emission coefficients are scaled with respect to their intensity. An analysis of the results obtained shows that, at the front of the propagating plasma bunch, a compression shock forms, within which chemical reactions of methane decomposition are initiated. At the fourth microsecond, the compression shock is detached from the plasma bunch. The observed intensification of the plasma flow at 7.6 μs is related to the second current pulse of the plasma generator. Then, the plasma expands and the reaction activity, as well as the intensity of plasma emission, decreases.

5. CONCLUSIONS

Tomographic reconstruction of the spatial structure and time evolution of the reagent zones on a microsecond time scale has been performed for the first time. It is found that, within a compression shock that forms at the front of a moving plasma bunch, chemical reactions of methane decomposition are initiated. Tomographic reconstruction has allowed us to determine the spatiotemporal evolution of the reagent zones and to examine how their behavior is related to the shock-wave structure arising in the interaction of a high-enthalpy plasma flow with a gaseous medium.

ACKNOWLEDGMENTS

This work was supported in part by the Presidium of the Russian Academy of Sciences (program no. P-09) and the Presidium of the Siberian Branch of the Russian Academy of Sciences (integration project no. 44).

REFERENCES

1. N. V. Denisova, G. Revalde, and A. Skudra, Fiz. Plazmy **32**, 1039 (2006) [Plasma Phys. Rep. **32**, 960 (2006)].
2. A. Kasperczuk and T. Pisarczyk, J. Tech. Phys. **58**, 521 (1997).
3. T. Neger, J. Phys. D **28**, 47 (1995).
4. N. V. Denisova, V. V. Pikalov, and A. L. Balandin, Opt. Spektrosk. **81**, 43 (1996) [Opt. Spectrosc. **81**, 41 (1996)].
5. N. V. Denisova, Opt. Spektrosk. **83**, 1019 (1997) [Opt. Spectrosc. **83**, 943 (1997)].

Translated by N.N. Ustinovskiĭ